Research Square

Preprints are preliminary reports that have not undergone peer review.
They should not be considered conclusive, used to inform clinical practice,
or referenced by the media as validated information.

Potassium Phosphite Modulated the Soil Microbiome and Enriched the Antagonistic Bacteria Streptomyces Coelicoflavus and Paenibacillus Favisporus to Inhibit the Tomato Pathogen Ralstonia Solanacearum Synergistically

Lv Su
NJAU
Xingxia Mo
NJAU
Juan Sun
NJAU
Pengfei Qiu
NJAU
Ruifu Zhang
NJAU
Eiko E. Kuramae
KNAW
Biao Shen (shenbiao@njau.edu.cn)
Nanjing Agricultural University https://orcid.org/0000-0002-5535-4389
Qirong Shen
NJAU

Research

Keywords: Agrochemical, Bacterial co-occurrences, Antagonistic strains, Streptomycin synthetic genes, Synergistic inhibition of Ralstonia solanacearum, Soil microbiome

Posted Date: January 13th, 2021

DOI: https://doi.org/10.21203/rs.3.rs-143372/v1

License: This work is licensed under a Creative Commons Attribution 4.0 International License.
Read Full License

Abstract

Background: Application of certain agricultural chemicals could modulate the soil microbiome and induce potential antagonistic microbes. However, the specific selective effects of agricultural chemicals on soil bacterial functions and their co-occurrences are not well understood, and no studies have verified that the enriched potential antagonistic microbes could enhance the antagonistic functions of the soil microbiome.

Results: Here, the effects of potassium phosphite (KP), an environment-friendly agricultural chemical, on the soil bacterial composition, co-occurrences and antagonistic functions were determined, and the potential antagonistic bacteria against the tomato bacterial wilt pathogen *Ralstonia solanacearum* were isolated to test their functions and associations among these strains. Our results showed that application of KP enriched *Bacillus*, *Paenibacillus* and *Streptomyces*. The positive links among the OTUs belonging to these genera were increased, and positive associations between these OTUs and predicted genes related to antagonistic substance production were revealed. Two strains, *Streptomyces coelicoflavus* F13 and *Paenibacillus favisporus* Y7, were isolated, and they inhibited the growth of *R. solanacearum*. Genomic sequencing showed that both strains harboured streptomycin synthetic genes, and *P. favisporus* Y7 also contained surfactin synthetic gene cluster. Synergistic inhibition of *R. solanacearum* growth by *P. favisporus* Y7 and *S. coelicoflavus* F13 was observed in soil. Genome-scale metabolic modelling showed that dextrin and lactic acid were potential cross-feeding metabolites. In addition, the KP-modulated soil microbiome could suppress *R. solanacearum* growth.

Conclusions: Our results highlight that a KP-modulated soil microbiome has considerable potential for biocontrol and indicate a new mechanism for the inhibition of *R. solanacearum* by KP-enriched soil bacteria.

Background

Tomato bacterial wilt is a serious disease caused by *Ralstonia solanacearum*. This vascular pathogen not only causes large economic losses annually but also leads to imbalanced bacterial communities [1, 2]. To manage tomato bacterial wilt disease, resistant cultivars, chemical bactericides and biocontrol agents have been used worldwide [3-5]. However, no effective methods have been found to control bacterial wilt, and prevention is still the major strategy. Moreover, after harvest, the root residuals in the soil provide the niche and nutrition for *R. solanacearum* to facilitate the next seasonal invasion [6]. Thus, decreasing the initial abundance of *R. solanacearum* may contribute to the prevention of bacterial wilt disease outbreak, for example, through the use of the fumigant chloropicrin [7]. However, this method is not environmentally friendly.

Agricultural chemicals are widely used in the control of soil-borne disease due to their direct inhibition of pathogens. The application of agricultural chemicals can significantly affect the soil microbial community [9]. Application of inorganic germicide copper depleted populations of bacteria, cellulolytic

fungal species and *Streptomyces* in sandy soil [10]. The application of another inorganic germicide, sulphur, enriched acidophilic soil bacteria [11]. Moreover, application of certain agricultural chemicals may enrich potential beneficial microbes in soil [12-14]. The relative abundances of the beneficial bacteria *Rhizobiales*, *Nitrosomonadaceae* and *Bryobacter* and functional genes related to nitrogen metabolism, carbohydrate metabolism and cell processes and the numbers of network modules were enriched in soil amended with selenium [15]. The application of chloropicrin fumigation increased the relative abundance of the potential antagonistic microbe Actinobacteria, which may result in an enhanced soil antibacterial capacity against *R. solanacearum* [7]. However, the effects of these agricultural chemicals on the soil microbial ecology, specifically for antagonistic functions and microbial associations are poorly understood. Furthermore, it is generally unknown whether the enriched beneficial bacteria could enhance the antagonistic ability of the soil microbiome.

Approximately 80% of antibiotics are known to be sourced from Actinobacteria [16]. *Streptomyces* has been widely used to suppress diverse plant pathogens in agricultural system [17, 18]. *Bacillus* species are known for their tremendous resistance to adversity and antagonistic capacities [19, 20]. Application of a *Bacillus amyloliquefaciens* strain that could produce iturin, fengycin and surfactin could effectively control tomato bacterial wilt, with a biocontrol efficiency of 97.6% [19]. Still, there is little understanding of whether the agricultural chemicals that were applied in soil can contribute to selective enrichment of *Streptomyces* and *Bacillus* strains that are beneficial for sustainable agricultural production.

Potassium phosphite (KP) has been used in agricultural systems and is receiving increasing attention because is environmentally friendly [21]. Several studies have shown that KP can control some soil-borne pathogens, such as bacterial wilt of geraniums caused by *R. solanacearum* [22] and *Fusarium* wilt in Monterey pines [23]. Moreover, KP can trigger the expression of host defence genes to resist plant pathogen invasion [24, 25] and directly inhibit the growth of pathogens, such as *Phytophthora* [26, 27]. The metabolic processes of *Phytophthora* related to phosphorus absorption are likely affected by KP. In addition, serval studies have shown that the application of phosphite can stimulate citrus yields [28] and increase the dry weights of the shoots and roots of cucumber plants [29]. Overall, KP may represent a promising chemical in agricultural systems.

Here, we determined the effects of KP on the composition, co-occurrence, and antagonistic functions of the soil bacterial community. Moreover, isolation and genomic analysis of potential antagonistic strains, determination of the antagonistic genes abundances as well as the associations of antagonistic strains, and a soil microbiome transfer experiment were performed, with the aims of identifying the agricultural chemicals that could contribute to selective enrichment of *Streptomyces* and *Bacillus* and of uncovering the mechanism of *R. solanacearum* inhibition by the enriched strains. We hypothesized that the KP-modulated soil microbiome may inhibit *R. solanacearum* indirectly.

Materials And Methods

The tomato bacterial wilt pathogen *R. solanacearum* ZJ3721 (biovar 3) used in the experiments was kindly provided by Professor Jianhua Guo; the KP solution was adjusted to a pH of 7.0 with potassium hydroxide; Luvisol soil (FAO) was collected from the upper soil layer (5-30 cm) of an open field covered with grass at the Experimental Base of Nanjing Agricultural University (32.01´N, 118.85´E). The soil characteristics are listed in the Supplementary methods (Table S5). Two other soils Luvisol soil (FAO) from a grape plantation of Hebei province (36.96´N, 115.39´E) were collected from the upper soil layer (5-30 cm) of an open field covered with grass (HN) and planted grape for two years (HG). All soils were air-dried and sieved (20 mesh).

Effects of KP on the soil bacterial community

The experiment included one treatment (soil amended with KP) and a control (CK) (Fig. 7). Approximately 75 ml of sterilized water was added to 1.5 kg of dry soil from Nanjing to wet the soil. Next, 150 ml of an *R. solanacearum* cell suspension (cell density: 8×10^6 cfu ml^{-1}) was added to the wet soil and mixed (final cell concentration: 8×10^5 cfu g^{-1} soil). *R. solanacearum*, as a soil-borne pathogen, can use root residuals to multiply; thus, tomato root tissues from healthy plants were added to the soils to simulate field conditions. Approximately 15 g of dry root tissues cut into approximately 1-mm lengths was added to 1.5 kg of soil at a rate of 1.0% (w/w) [42]. Then, 750 g of soil containing root tissues was taken as the treatment and control. KP was applied at a concentration of 0.5% (w/w) [22] (KP treatment). The soil moisture of both the control and the KP treatments was adjusted to 45% of the soil capacity. Then, 750 g of soil was divided into 25 replicates consisting of 30 g of soil in a 50 ml centrifuge tube and then incubated at 30°C. The soils from the three replicates were randomly taken from all samples on days 7, 14 and 30 for soil DNA extraction.

The effects of KP on the numbers of culturable Actinobacteria were performed in two other soils (HN and HG). The same processes for the effects of KP on the microbial community of soil from Nanjing were performed. The three replicates from the two soils were randomly taken on days 7. One gram of the sampled soils was diluted and then spread on gauze No. 1 agar plates. The plates were incubated for 5 days at 28°C, and the numbers of culturable Actinobacteria were determined.

DNA isolation and Illumina HiSeq of the soil DNA

Total soil DNA was extracted using the PowerSoil® DNA Isolation Kit (MOBIO Laboratories, Carlsbad, CA, USA) according to the manufacturer's instructions.

The V4 hypervariable regions of the 16S rRNA gene were amplified using primers 515F (5-GTGCCAGCMGCCGCGGTAA-3) and 907R (5-CCGTCAATTCCTTTGAGTTT-3). Subsequently, 0.4 μl of the primers and approximately 10 ng of template DNA were analysed via PCR with the following thermal cycling conditions: an initial denaturation at 98°C for 1 min, followed by 30 cycles of denaturation at 98°C for 10 s, annealing at 50°C for 30 s, and extension at 72°C for 60 s, with a final extension step at 72°C for 5 min after the cycling was complete. The PCR products were detected by electrophoresis in 1% (w/v) agarose gel and then purified with the GeneJET Gel Extraction Kit (Thermo Scientific). The purified

PCR amplicons were sequenced using the Illumina HiSeq (250-bp paired-end reads) platform at the Novogene Bioinformatics Technology Co., Ltd. (Beijing, China).

The sequencing data were mainly processed on the USEARCH platform [43]. Briefly, sequences with a quality score lower than 0.5 or a length shorter than 200 nt and singletons were discarded. Noisy sequences were filtered, chimerism was inspected and an OTU cutoff was assigned at the 97% identity level. Representative sequences for each OTU were selected and classified according to the RDP database for bacteria (cutoff = 80%). To correct for differences in the sequencing depth, the bacterial read counts were rarefied to the lowest number of sequences present in each sample set. The raw sequences were submitted to the NCBI Sequence Read Archive (SRA) under BioProject accession PRJNA577427.

The functional genes of the bacterial community were predicted by PICRUSt [44]. The 16S sequences were used for closed-reference OTU selection with QIIME [45]. The resulting OTU table was used to predict the functional genes based on the metagenome inference workflow.

Bacterial isolation and Sanger sequencing of 16S rRNA genes

The sampled soil at 7 days from the KP treatment was serially diluted and then spread on nutrient agar (NA) and gauze No. 1 agar plates. The plates were incubated for 3-5 days at 28°C. Because our target microbes are dominant taxa in the results of high-throughput sequencing, 33 dominant colonies (numbers of similar morphology > 5 in each plate) were selected. A loop of bacterial cells was added to 500 μl of water and incubated for 15 min at 95°C. Next, the cells were cooled on ice for 1 min and centrifuged at 10,000 × g for 1 min to remove the cell debris. The supernatant of the cell lysate was used as a DNA template for the amplification of the 16S rRNA genes. Information on the detailed primers F27 and R1492 and the PCR steps are listed in Table S6 and Table S7, respectively. Sanger sequencing was performed by the Qin Ke Company (Nanjing, China). The sequences of these bacteria were classified against the 16S ribosomal RNA database using NCBI BLAST. The 16S rRNA sequences of the isolates were clustered to the OTUs at 100% sequence similarity in USEARCH.

Draft genomes of two strains of bacteria identified as *Paenibacillus favisporus* Y7 and *Streptomyces coelicoflavus* F13

The genomes of the two isolates *Paenibacillus favisporus* Y7 and *Streptomyces coelicoflavus* F13, which were highly abundant in the microbial community of the KP-treated soil, were sequenced. The sequences were analysed according to the method described in a previous study [46]. Briefly, the low-quality sequences were removed by adapter removal (version 2.1.7). After filtering, a total of 9,141,712 (98.65%) and 16,401,350 (97.68%) high-quality paired-end reads were obtained for strains Y7 and F13, respectively. All reads were quality corrected by SOAPec (version 2.0) based on the k-mer frequency, with the k-mer used for correction set to 17. The genome was assembled *de novo* using A5-miseq (version 20150522). The draft genome sequences of strains Y7 and F13 contained 17 and 59 contigs (a sequence length greater than 1 kb), respectively. The coding DNA sequences (CDs) in the draft genomes were predicted by GeneMarkS (version 4.32). The predicted CDs were searched against the NCBI NR protein database and

the Kyoto Encyclopedia of Genes and Genomes (KEGG). The whole-genome shotgun project has been deposited in GenBank under the accession number WIBG00000000 (strain Y7) and WFLH00000000 (strain F13).

Effect of KP on the growth of *R. solanacearum*,*P. favisporus* Y7 and *S. coelicoflavus* F13 *in vitro*

To measure the cell density (OD_{600}) under KP conditions, 200 µl of *R. solanacearum* (approximately 10^8 cfu ml^{-1}) and *P. favisporus* Y7 (approximately 10^8 cfu ml^{-1}) was inoculated in 3 ml of LB (Luria Broth) liquid containing KP at a concentration of 0.5%. To measure the dry biomass of F13 under KP conditions, 200 µl of *S. coelicoflavus* F13 spores (approximately 10^8 cfu ml^{-1}) was inoculated in 20 ml of LB liquid containing KP at a concentration of 0.5%. The LB liquid without KP was used as the control. Each treatment had four replicates. After 48 h of incubation at 30°C (*R. solanacearum* and *P. favisporus* Y7) and 28°C (*S. coelicoflavus* F13) and 170 rpm, the cell densities (OD_{600}) of *R. solanacearum* and strain Y7 and the dry biomass of strain F13 were measured.

Inhibition of *R. solanacearum* growth by *P. favisporus* Y7 and *S. coelicoflavus* F13 *in vitro*

Approximately 2 µl of the strain Y7 cell suspension (cell density: 10^8 cfu ml^{-1}) and 5-mm-diameter agar plugs of strain F13 grown in gauze No. 1 agar plates for 5 days were spotted onto the centre of NA medium agar plates and incubated at 30°C (strain Y7) and 28°C (strain F13) for three days. Then, 200 µl of *R. solanacearum* (cell density: 10^7 cfu ml^{-1}) was sprayed onto the plates. After 48 h of incubation at 30°C, the inhibition diameters of the two strains were measured with a ruler. Each treatment had three replicates.

Mutual stimulation between strains *S. coelicoflavus*F13 and *P. favisporus*Y7 *in vitro*

Strain *P. favisporus* Y7 and strain *S. coelicoflavus* F13 were cultured in 200 ml of one-tenth LB liquid at 30°C (strain Y7) for 2 days and 28°C (strain F13) for 5 days, respectively, at 170 rpm. Then, the culture suspensions were centrifuged at 10,000 × g for 5 min. The supernatants were sterilized with 0.22-mm sterile filter membranes. Next, 20 µl of cell suspensions of strains Y7 (approximately $1×10^8$ cfu ml^{-1}) was inoculated in 3 ml of one-tenth LB liquid containing the sterilized supernatants of strains F13 at concentrations of 10%, 30% and 50% (v/v). Approximately 20 µl of spore suspensions of F13 (approximately $1×10^8$ cfu ml^{-1}) was inoculated in 20 ml of one-tenth LB liquid containing the sterilized supernatants of strains Y7 at concentrations of 10%, 30% and 50% (v/v). The one-tenth LB liquid without strain supernatants was used as the control. Each treatment had four replicates. After 24 h of incubation at 30°C (strain Y7) and 28°C (strain F13) at 170 rpm, the cell density (OD_{600}) of strain Y7 and the dry biomass of strain F13 were measured.

Inhibition of *R. solanacearum* by combined *P. favisporus* Y7 and *S. coelicoflavus* F13 in sterile soil

Approximately 50 ml of sterilized water was added to 1 kg of dry sterilized soil (2 × 99 min at 121 °C) to wet the soil. Approximately 50 ml of the *R. solanacearum* cell suspension (cell density at $2×10^6$ cfu ml^{-1})

and 10 g of sterilized root tissues (approximately 1 mm lengths) were added to the wet soils and mixed (final *R. solanacearum* concentration of 1×10^5 cfu g^{-1} dry soil). Then, all soils were divided evenly into 6 parts (per part: 166 g). Approximately 10 ml of the spore suspension of strain F13 at 1.66×10^6 cfu ml^{-1} (part 1), 10 ml of strain Y7 at 1.66×10^6 cfu ml^{-1} (part 2) and combinations of Y7 and F13 at different inoculation concentrations (Y7: F13 = 7:3 (part 3), 5:5 (part 4), 3:7 (part 5)) were added to the 166 g of soil to a final density of 1×10^5 cfu g^{-1} dry soil. Approximately 10 ml of sterile water was added to 166 g of soil as a control (part 6). Before being added to the soil, all strains were washed 5 times. Approximately 30 g of the soil from each part was placed in a 50-ml sterilized centrifuge tube with 5 replicates and incubated at 30°C for 20 days; then, the soil samples were used for DNA extraction.

Inhibition of *R. solanacearum* by the KP-modulated soil microbiome

A soil microbiome transfer experiment was performed to determine the function of the KP-modulated soil microbiome. The soil microbiome transfer experiment was performed based on a previous study [47] with slight modifications. The same processes for determining the effects of KP on the soil microbial community were performed but without the addition of *R. solanacearum* in the soil from Nanjing. On day 7, 5 g of KP-treated soil and control soil were added separately to 45 ml of sterile water in a flask on a shaker at 200 rpm for 30 min followed by sonification for 1 min at 47 kHz twice with shaking for another 30 min. Next, the soil suspension of each treatment was filtered with sterile filter paper (15 μm pore size) to remove soil particles. To remove water-soluble nutrients/chemicals, such as KP, the filtrate was centrifuged at 3,000 × g for 30 min, and the supernatant was discarded. The pelleted microorganisms were resuspended in 5 ml of sterile water.

Approximately 20 ml of sterilized water was added to 360 g of dry sterilized soil (2 × 99 min at 121 °C) to wet the soil; this soil was mixed with 9 ml of the *R. solanacearum* cell suspension (cell density at 8×10^7 cfu ml^{-1}) and 3.6 g of dry sterilized tomato root tissues (approximately 1-mm lengths) and then divided evenly into 2 parts. Then, 3 ml of the cell suspension extracted from the KP treatment and control soils was applied separately to 180 g of sterilized soil containing root tissues. Each 180-g sample of the above soil was divided into 6 replicates of 30 g each in 50-ml sterilized centrifuge tubes, referred to as the MK microbial community from the KP-treated soil (MK) or the microbial community from the control soil (MC) treatments, and then incubated at 30°C. The soils from three replicates were randomly sampled on day 20 [48] for DNA extraction.

Quantitative PCR to measure the copies of functional genes

The copy numbers of the *fliC* (*R. solanacearum*), 16S rRNA (total bacteria), con31_49 (*S. coelicoflavus* F13), con2_67 (*P. favisporus* Y7), the main antagonistic genes for *Bacillus* (*srf* (surfactin), *itu* (iturin) and *fen* (fengycin)) were quantified by quantitative PCR. After sequencing the genomes of *S. coelicoflavus* and strain *P. favisporus*, the unknown functional genes from contig31_6449 (strain *S. coelicoflavus*) and contig2_3067 (strain *P. favisporus*) were found without homologous genes in the NCBI. Thus, the gene fragments were used to design primers (con31_49 for *S. coelicoflavus* and con2_67 for *P. favisporus*) in

Premier 5. The designed primers were tested by primer-blast (www.ncbi.nlm.nih.gov/tools/primer-blast/), and no microbes were obtained.

Quantitative PCR (qPCR) assays were performed using the SYBR Premix Ex Taq^{TM} (Perfect Real-Time) Kit (Takara Biotechnology Co., Dalian, China) with the ABI StepOne^{TM} Real-Time PCR System (Applied Biosystems, USA). Each reaction was performed in a 20 μl volume. The detailed primer information and PCR steps are listed in the supporting information (Table S6 and Table S7). Standard curves were developed by serially diluting the plasmids with known positive inserts to final concentrations of 10^2 to 10^7 gene copies μl^{-1}. The QPCR efficiencies ranged from 90% to 105%, and the R^2 values for all four assays were greater than 0.99.

Data analysis

The OTU tables were converted into a suitable input file for bacterial diversity analysis using Mothur [49]. Principal coordinate analysis (PCoA) of the bacterial community structure was performed by calculating the Bray-Curtis dissimilarity in R. Differences between groups were tested for significance by a permutation-based analysis of variance by using the adonis function of the vegan package in R. The significant genera (top50) between the control and the KP treatment and the MC and MK treatments were identified with DESeq in R, and the significant genera were shown in a circular treemap using the ggraph package in R.

Significant differences in the bacterial community diversity indices, the number of culturable Actinobacteria, the number of functional gene copies, colony diameters, inhibition zone diameters, the cell densities (OD_{600}) of *R. solanacearum* and strain *P. favisporus* Y7 and the biomass of strain *S. coelicoflavus* F13 from the inhibition level results were assessed using Student's t test; the data conformed to a normal distribution according to the Shapiro-Wilk test in R. Significant differences in the relative abundance levels of the PICRUSt-predicted genes were assessed using Welch's t-test.

The data on the cell density (OD_{600}) of strain *P. favisporus* Y7 and the biomass of strain *S. coelicoflavus* F13 from the mutual stimulation results were subjected to one-way ANOVA and then Tukey's test for multiple comparisons.

The OTU abundances (top 300) were used to build a microbial network by the function sparcc with 100 permutations in Mothur software. Edges whose p.adjust value was < 0.001 were retained. The link number of nodes (OTU degree) and visualized networks were assessed using Gephi software [50]. Phylogenetic trees of nodes were built by MEGA7. Moreover, the associations between the relative abundances of hubs (link numbers >50) from bacterial networks and the predicted genes related to production of antagonistic substances were determined by the cor.test function in R with the "pearson" method. The p-values were adjusted by the "FDR" method.

The gene annotation protein.faa files of strains Y7 and F13 were used to construct genome-scale metabolic models with "carve" functions, and the genome-scale metabolic models of strains Y7 and F13

were used to generate the microbial community models with the “merge_community” functions by CarveMe [51]. The metabolic substances and reactions of the microbial community models were obtained by the sybilSBML package in R, and the associations between metabolic substances and reactions were visualized using Cytoscape software [52].

Results

Effects of KP on *R. solanacearum*, total bacteria and the soil bacterial community

The copy numbers of the *fliC* (representing *R. solanacearum*) and 16S rRNA genes (representing total bacteria) were significantly reduced by approximately 1.91-fold to 2.44-fold and 1.61-fold to 4.81-fold, respectively, at all sampling times in the KP treatment (Fig. 1a and Fig. 1b). The Shannon diversity of the soil bacterial community was slightly decreased in the soil amended with KP on days 7 and 14 (Fig. S1); however, the diversity was recovered at day 30. The microbial community structure of the control at different sampling times was significantly different from that of the KP treatment ($P = 0.001$, $R = 0.45$) (Fig. 1c). The difference in bacterial community structure between the control and KP treatment at day 7 was greater than that at days 14 and 30. Moreover, the bacterial community structure of the control at day 7 was different from that at days 14 and 30, suggesting that the time factor of tomato root residuals significantly affected the soil bacterial community.

Actinobacteria, Proteobacteria, Firmicutes and Bacteroidetes were the dominant phyla in the bacterial communities (Fig. S2). Actinobacteria (56.93%) was enriched, but Proteobacteria (16.21%) and Bacteroidetes (2.67%) were depleted in the KP treatment at days 7 and 14. However, the relative abundance of Proteobacteria (30.63%) in the KP treatment was higher than that in the control at day 30. To increase the robustness of our results, we determined the number of culturable Actinobacteria in two other soils supplemented with KP. The numbers of culturable Actinobacteria in the HN and HG soils amended with 0.5% KP were 1.5-fold and 1.4-fold higher than those in the corresponding controls, respectively (Fig. S3).

At the genus level, the relative abundance of the dominant bacterium *Streptomyces* (25.29%) was significantly increased in the KP treatment for all sampling days (Fig. 1d, Fig. S4 and Fig. S5). *Paenibacillus* was significantly enriched in the KP treatment at days 7 and 14 (Fig. 1d and Fig. S4). *Bacillus* was significantly enriched in the KP treatment only at day 7 (Fig. 1d). Specifically, in addition to *Micromonospora*, *Arthrobacter*, *Agromyces* and *Sporosarcina*, the other significantly changed genera (top 50) belonging to Actinobacteria and Firmicutes, such as *Actinoallomurus* and *Actinocatenispora*, were significantly enriched in the KP treatment at day 7 (Fig. 1d). In addition to *Sphingomonas*, the other significantly changed genera (top 50) belonging to Bacteroidetes and Proteobacteria, such as *Massilia* and *Flavobacterium*, were significantly depleted in the KP treatment at day 7 (Fig. 1d). However, *Bacillus* and *Flavobacterium* were significant depleted and enriched in the KP treatment at day 14 and 30, respectively (Fig. S4 and Fig. S5). Moreover, *Sphingobium*, *Chitinophaga* and *Ensifer* were significantly depleted in the soil of the KP treatment at all sampling times.

Effect of KP on the co-occurrence networks of the soil bacterial community

Because of the difference in the composition of the bacterial community, we compared the bacterial networks between the KP treatment and control. The results showed that KP application slightly increased the link number of the bacteria community co-occurrence networks (Fig. S6).

The nodes with > 50 links represented hubs in the bacterial network. The top 10 hubs are shown in Table S1. We found that the OTUs belonging to *Streptomyces*, *Paenibacillus* and *Bacillus* had the greatest link numbers. The link number of OTUs (*Bacillus*) was greatly higher in the KP treatment than in control, while the link number of OTUs (*Paenibacillus* and *Streptomyces*) was slightly lower in the KP treatment.

Due to the fact that *Streptomyces*, *Paenibacillus* and *Bacillus* were the dominant potential antagonistic bacteria and the top hubs, the associations between these potential antagonistic bacteria and other bacteria were determine. Unless otherwise noted, the target hub (link number > 50) refers hereafter to the nodes belonging to the potential antagonistic bacteria (*Streptomyces*, *Paenibacillus* and *Bacillus*). Our results showed that the positive links between the target hubs and nodes belonging to Actinobacteria and Firmicutes (not including *Streptomyces*, *Paenibacillus* and *Bacillus*) were increased 1.73-fold and 1.22-fold, but the relative abundances of these nodes were decreased 1.36-fold and 2.28-fold in the bacterial network of KP treatment compared to those in the control network (Table S2). The low and high relative abundances of nodes that have positive associations with the target hubs were increased and decreased, respectively, in the bacterial network of KP treatment (Fig. S7). In addition, the opposite results were found in the negative links between the target hubs and these nodes (Table S3 and Fig. S4). These results suggested that the dominant target hubs may enhance the cooperation and competition with rare and dominant bacteria, respectively.

The associations between target hubs and the nodes belonging to Proteobacteria and Bacteroidetes were determined. We found that both the negative and positive link numbers between the nodes (Proteobacteria and Bacteroidetes) and the target hubs were decreased, suggesting that certain low-abundance bacteria belonging to Proteobacteria and Bacteroidetes may disappear with KP treatment, resulting in the decreased link numbers of these nodes (Table S2 and S3). In addition, the relative abundances of both rare and dominant nodes (Proteobacteria and Bacteroidetes) that had negative and positive links to the target hubs were also decreased in the KP-treated soil, suggesting that the target hubs corresponding to the potential antagonistic bacteria may inhibit the growth of the bacteria belonging to Proteobacteria and Bacteroidetes.

The associations among these target hubs showed that the numbers of the target hubs were increased 1.5-fold, and the positive link numbers among the associations of themselves were increased 3.19-fold in the KP-treated soil compared to those in the control soil (Fig. 2). Moreover, the relative abundances of the increased target hubs from the KP treatment were significantly lower by approximately 4.9-fold to 199.6-fold than those of the dominant target hub (*Streptomyces*_OTU1). In summary, KP may enhance the cooperative associations among these target hubs.

The associations between the target hubs and predicted antagonistic genes from PICRUST were determined (Fig. S8). In addition to OTU38 (*Streptomyces*), the other OTUs (*Streptomyces*) and OTU39 (*Paenibacillus*), whose link numbers were more than 50, had significant and positive associations with the predicted antagonistic genes related to biosynthesis of 14-membered macrolides, type II polyketide products, vancomycin, butirosin, penicillin, and streptomycin, suggesting that these OTUs corresponded to bacteria that could produce these antagonistic substances. However, positive associations were not found between the OTUs (*Bacillus*) and these genes related to the biosynthesis of antagonistic substances described above.

Isolation and characterization of potential antagonistic microbes in soil

To test the results related to the positive associations among the target hubs and their antagonistic functions, we isolated 33 dominant strains from the KP-treatment soil and found OTU1 and OTU39, for which the sequences were clustered to the 16S rRNA sequences of the strains F13 (*Streptomyces coelicoflavus*) and Y7 (*Paenibacillus favisporus*) at 100% sequence similarity (Fig. 3). q-PCR results showed that the copy numbers of the specific gene fragments con31_49 of *S. coelicoflavus* F13 and con2_67 of *P. favisporus* Y7 were significantly higher in the KP treatments than in the control ($P = 0.01$) at three sampling times (Fig. 3b), which confirmed the enrichment of the strains *S. coelicoflavus* F13 and *P. favisporus* Y7 in the soil amended with KP.

Based on the enrichment of the isolates *P. favisporus* Y7 and *S. coelicoflavus* F13 and the depletion of *R. solanacearum* in the KP treatment, we speculated that the inhibition levels of *R. solanacearum*, *P. favisporus* Y7 and *S. coelicoflavus* F13 by KP were different. Indeed, *R. solanacearum* barely grew in LB liquid medium amended with KP at a concentration of 0.5% (Fig. S9). KP also inhibited the growth of *P. favisporus* Y7 and *S. coelicoflavus* F13 *in vitro*, but the inhibition levels of *P. favisporus* Y7 and *S. coelicoflavus* F13 by KP were much lower than that of *R. solanacearum*.

We determined whether the enriched isolates *P. favisporus* Y7 and *S. coelicoflavus* F13 could inhibit *R. solanacearum* growth *in vitro*. Indeed, obvious inhibition zones of *P. favisporus* Y7 and *S. coelicoflavus* F13 to *R. solanacearum* were found on NA plates (Fig. S10).

Because a positive association between OTU1 (*Streptomyces*) and OTU39 (*Paenibacillus*) was found in the bacterial networks of KP treatment, we speculated that *S. coelicoflavus* F13 and *P. favisporus* Y7 may form a mutualistic association to inhibit the growth of *R. solanacearum*. The results showed that the fermentation broth of *S. coelicoflavus* F13 could significantly stimulate the growth of *P. favisporus* Y7 at all tested concentrations ($P < 0.001$), and the highest stimulation of *P. favisporus* Y7 was found at a concentration of 30% (v/v) fermentation broth of *S. coelicoflavus* F13 (Fig. S11). Similarly, the growth of *S. coelicoflavus* F13 was stimulated by the fermentation broth of *P. favisporus* Y7 at three tested concentrations. In addition, the cell suspension of *S. coelicoflavus* F13 was more homogeneous in LB liquid medium amended with the fermentation broth of *P. favisporus* Y7 than in the control.

Functional analysis based on the genomes of *P. favisporus* Y7 and *S. coelicoflavus* F13

We further determined the functions of the isolates from their genomes to support the above results. Due to their antagonistic ability against *R. solanacearum*, the KEGG metabolic pathways of the biosynthesis of other secondary metabolites (Fig. 4) were considered. The results showed that both strains contained the metabolic pathways related to the biosynthesis of prodigiosin, monobactam, streptomycin, phenylphopaniod and validamycin. Specifically, the contig numbers of streptomycin biosynthesis were the highest in both strains. The operon (*rfbA*, *rfbB*, *rfbC* and *rfbD*) that encodes dTDP-L-rhamnose, which is an important branch related to the production of dTDP-L-dihydrostreptose in streptomycin biosynthesis, was found in both strains. Furthermore, distinct genes related to the production of surfactin for *P. favisporus* Y7 and germicidin and toxoflavin for *S. coelicoflavus* F13 were found (Table S4).

Because the antagonistic gene *stfAB* was found in the genome of *P. favisporus* Y7, we speculated that these genes related to the production of surfactin were enriched in the soil amended with KP. Thus, the copy numbers of three genes related to the production of the main lipopeptides (*srf*, *itu* and *fen*) were determined in the soil (Fig. S12). We found that the copy numbers of *srf*, *itu* and *fen* were approximately 2.22-fold to 3.51-fold higher in the KP treatment than in the control at 7 days. Similar differences in the copy numbers of the antagonistic genes were found at 14 and 30 days between the KP treatment and control.

Because of the mutualistic associations between strain F13 and Y7, we constructed a genome-scale metabolic model of strains F13 and Y7 to identify cross-feeding metabolites. In general, cross-feeding metabolites are produced by one microbe and utilized by another microbe in extracellular environments. Thus, we focused on the metabolic reactions in extracellular environments. The results showed that 312 metabolic reactions were existed in both strain F13 and Y7, suggesting that certain nutrients could be utilized by both strains. Moreover, 134 and 55 distinct metabolic reactions were found in strains F13 and Y7, respectively, suggesting that certain distinct metabolites could be produced (Fig. S13). The detailed metabolites in extracellular environments were further determined, and the results showed that 65 main carbon and nitrogen sources, specifically, cellobiose and xylobiose, could be utilized by both strains (Fig. S14). Both strains harbour the operon (*xylA*, *xylB* and *xylD*) for D-xylose metabolism, suggesting that both strains can use certain nutrients from soil root residuals (Fig. S15 and Fig. S16). Moreover, dextrin could be produced via alpha amylase reaction in strain F13 and utilized by strain Y7 for dextrin transport via proton symport and maltodextrin glucosidase dextrin reactions (Fig. 5). L-lactate could be produced via lactaldehyde dehydrogenase in strain Y7 and utilized by strain F13 for lactate reversible transport via proton symport, L-lactate dehydrogenase and tagatose 1,6-diphosphate aldolase reactions.

Synergistic inhibition of *R. solanacearum* by Antagonistic strains Y7 and F13 in soil

Since the cross-feeding existed between strain Y7 and strain F13, a soil culture experiment was performed to determine whether strains Y7 and F13 could inhibit *R. solanacearum* synergistically at different inoculation rates. According to the results of the soil culture experiment, *P. favisporus* Y7 and *S. coelicoflavus* F13 in combination or alone could significantly inhibit *R. solanacearum* growth in a sterile soil (Fig. S17). *S. coelicoflavus* F13 exhibited less inhibition than *P. favisporus* Y7. In addition, the lowest

copy number of *fliC* was found in the soil amended with *P. favisporus* Y7 and *S. coelicoflavus* F13 at an inoculation ratio of 7 to 3, suggesting that synergistic inhibition of *R. solanacearum* existed.

Inhibition of *R. solanacearum* by the KP-modulated soil microbiome

As the antagonistic bacteria *Streptomyces* and *Paenibacillus* were highly enriched in the soil amended with KP at 7 days, we speculated that the KP-modulated microbiome from 7 days may inhibit the growth of *R. solanacearum*. The results showed that the copy number of *fliC* (*R. solanacearum*) was significantly lower by approximately 1.38-fold in the MK treatment (the soil amended with the microbiome from the KP treatment) than in the MC treatment (the soil amended with the microbiome from the control) ($P = 0.004$) (Fig. S18a). The qPCR results showed that the copy number of the specific gene fragments con31_49 of *S. coelicoflavus* F13 and con2_67 of *P. favisporus* Y7 were significantly higher in the MK than MC treatments ($P = 0.01$) (Fig. S18b and c).

Discussion

KP affected the composition of the soil bacterial community

KP, as an environment-friendly compound, is attracting increasing attention. Previous studies have focused on the function of KP in the induction of host resistance and the inhibition of pathogen growth [30]. In our study, we found that the relative abundance levels of Actinobacteria were increased, but Proteobacteria and Bacteroidetes were decreased in the soil amended with KP (Fig. S2). In agreement with our study, when the fungicide azoxystrobin was added to soil, the relative abundance of Actinobacteria was significantly increased [14]. The application of metam sodium fumigation could enrich the potential antagonistic microbes *Actinomycetales* and *Bacilli* [13]. However, *Micromonospora* and *Sporosarcina* belonging to Actinobacteria and Firmicutes, respectively, were significantly depleted in the KP-treated soil. It was possible that the enriched bacteria may indirectly inhibit the growth of *Micromonospora* and *Sporosarcina*. In addition, the differences in bacterial community structure were gradually decreased between the control and KP treatment from days 7 to 30, suggesting that the KP-modulated soil bacterial community could be gradually recovered (Fig. 1c). Likely, KP was gradually converted to phosphate in soil as a result of soil microbial activity [31].

KP affected the networks and antagonistic functions of the soil bacterial community

In our study, the numbers of positive links these target hubs were increased in the bacterial network of KP-treated soil, and the relative abundances of increased hubs in the KP treatment were much lower than that of the target hub OTU1 (*Streptomyces*) (Fig. 2). Similar results were also found in the positive associations between target hubs and the nodes belonging to Actinobacteria and Firmicutes (not including the target hubs) (Fig. S7), suggesting that a substantial content of metabolites from the dominant bacteria may have positive effects on the non-dominant bacteria. KeheJ et al. tested the associations among 60 strains and found that positive interactions commonly occurred between dominant and non-dominant bacteria [32]. Moreover, the relative abundances of the OTUs belonging to

Proteobacteria and Bacteroides that had negative associations with the target hubs were significantly decreased in the KP treatment. In addition, the positive associations between certain target hubs, such as OTU1 (*Streptomyces*) and OTU39 (*Paenibacillus*), and the predicated antagonistic genes were found in the KP-treated soil (Fig. S8). This result suggested that the bacteria belonging to these target hubs may inhibit the growth of bacteria belonging to Proteobacteria and Bacteroides. In line with our study, the application of glucose and fructose in soil resulted in *Streptomyces* populations with greater niche widths and selectively enriched *Streptomyces* antagonistic phenotypes to inhibit the nutrient competitors [33]. In summary, application of KP may enrich the symbiotic antagonistic bacteria that play important roles in modulating the soil microbiome.

KP induced the antagonistic bacteria *S. coelicoflavus* F13 and *P. favisporus* Y7 to inhibit the growth of *R. solanacearum* synergistically

To support the above results, we isolated 33 dominant strains in the soil amended with KP and found that *S. coelicoflavus* F13 and *P. favisporus* Y7 had stronger tolerance to KP than *R. solanacearum* (Fig. S9). The previous study showed that because *Microcystis aeruginosa* (*Cyanobacteria*) had stronger tolerance to the fungicide azoxystrobin than *Chlorella pyrenoidosa* (*Chlorella*), azoxystrobin could favour *M. aeruginosa* growth through growth inhibition of *C. pyrenoidosa* in a freshwater ecosystem [34]. Most likely, the microbes that were susceptible to KP were depleted, and their niches were occupied by *S. coelicoflavus* F13 and *P. favisporus* Y7, which may be the main reason for the enrichment in the KP-treated soil. In addition, *S. coelicoflavus* F13 and *P. favisporus* Y7 (gram-positive bacteria) form a thick and dense peptidoglycan layer, and this layer may play an important role in resisting adversity. In agreement with our study, the application of metalaxyl had a transient stimulation effect on Actinomycetes [12]. On the other hand, both strains (F13 and Y7) contained genes related to the utilization of D-xylose, which may have helped them to occupy many niches in the soil amended with root residues (Fig. S15 and Fig. S16).

A previous study has shown that *S. coelicoflavus* can produce 1H-pyrrole-2-carboxylic acid to inhibit the quorum sensing of *Pseudomonas aeruginosa* [35]. *P. favisporus* isolated from the tomato phyllosphere can induce resistance in tomato plants to suppress root rot [36]. However, no previous studies have shown that these two bacteria can inhibit the growth of the tomato pathogen *R. solanacearum*. In our study, antagonistic genes related to the synthesis of streptomycin were found in *P. favisporus* Y7 and *S. coelicoflavus* F13 (Fig. 4), which was in line with the results from the predicated function of the soil microbiome. Streptomycin sulphate has been used to manage tomato bacterial wilt disease [37]. Antagonistic genes in *P. favisporus* Y7 related to the synthesis of surfactin, which can inhibit the growth of *R. solanacearum* [38], were also found. Indeed, the copy number of *srf* (surfactin) was significantly increased with KP treatment (Fig. S12). Moreover, certain antagonistic genes of *Bacillus* related to the production of other lipopeptides, such as iturin and fengycin, were also enriched in the soil of KP treatment, suggesting that other potential antagonistic *Bacillus* species may be enriched. Moreover, the genome-scale metabolic model showed that the distinct metabolites dextrin and lactic acid could be produced by strain Y7 and strain F13, respectively, and utilized by strain F13 and strain Y7, respectively

(Fig. 5) that may be the main reason for in the synergistic inhibition of *R. solanacearum* by strain F13 and strain Y7. Moreover, the KP-modulated soil microbiome cultivated in sterile soil could also inhibit the growth of *R. solanacearum* (Fig. S18), supporting the above results. Overall, a model was proposed that the symbiotic antagonistic bacteria *S. coelicoflavus* F13 and *P. favisporus* Y7 were enriched in soil amended with KP, resulting in the inhibition of *R. solanacearum* indirectly (Fig. 6).

Conclusion

Here, we showed that KP application enriched the potential antagonistic genera *Streptomyces* and *Paenibacillus* and enhanced the positive associations among these potential antagonistic genera as well as the antagonistic functions of the soil microbiome. Moreover, two antagonistic strains whose 16S RNA sequences were clustered to OTU1 (*Streptomyces*) and OTU39 (*Paenibacillus*) have stronger tolerance to KP than *R. solanacearum*. In addition, both strains have genes related to the production of streptomycin. The mutual stimulation between *P. favisporus* Y7 and *S. coelicoflavus* F13 *in vitro* may result in synergistic inhibition of *R. solanacearum* growth. The results of genome-scale metabolic modelling showed that dextrin and lactic acid were potential cross-feeding metabolites. Furthermore, the KP-modulated soil microbiome could suppress the growth of *R. solanacearum*. The results of this study suggest that the KP-modulated soil microbiome has considerable potential for biocontrol and indicate a new mechanism for inhibition of *R. solanacearum* by KP-enriched soil bacteria.

Declarations

Acknowledgements

This work was supported by the Chinese Natural Science Fund Program (41571242). The authors thank Ms. Chao Zhou and Ms. Zhenghua Wu for technical assistance. Publication number XXXX of the Netherlands Institute of Ecology (NIOO-KNAW).

Funding

This work was supported by the Chinese Natural Science Fund Program (41571242).

Authors' contributions

Lv Su conceived the project and performed almost all experiments except for the following. Xingxia Mo and Juan Sun isolated strains from soils. Pengfei Qiu extracted soil DNA. Lv Su analysed all experimental data and composed the main text. Eiko E. Kuramae and Ruifu Zhang provided suggestions for the manuscript. Biao Shen and Qirong Shen organized and supervised the project, respectively.

Ethics approval and consent to participate

Not applicable.

Competing interests

The authors declare that they have no competing interests.

References

1. Hayward AC: **Biology and Epidemiology of Bacterial Wilt Caused by *Pseudomonas Solanacearum*.** *Phytopathology* 1991, **29:**65-87.
2. Wei Z, Hu J, Gu Ya, Yin S, Xu Y, Jousset A, Shen Q, Friman V-P: ***Ralstonia solanacearum* pathogen disrupts bacterial rhizosphere microbiome during an invasion.** *Soil Biology and Biochemistry* 2018, **118:**8-17.
3. Fock I, Collonnier C, Purwito A, Luisetti J, Souvannavong V, Vedel F, Servaes A, Ambroise A, Kodja H, Ducreux G: **Resistance to bacterial wilt in somatic hybrids between *Solanum tuberosum* and *Solanum phureja*.** *Plant Science* 2000, **160:**165-176.
4. Hong JC, Timur MM, Ji P, Olson SM, Colee J, Jones JB: **Management of bacterial wilt in tomatoes with thymol and acibenzolar-S-methyl.** *Crop Protection* 2011, **30:**1340-1345.
5. Chen D, Li C, Wu K, Xun G, Yuan S, Shen Q, Shen B: **A phcA − marker-free mutant of *Ralstonia solanacearum* as potential biocontrol agent of tomato bacterial wilt.** *Biological Control* 2015, **80:**96-102.
6. Yadeta K, Thomma B: **The xylem as battleground for plant hosts and vascular wilt pathogens.** *Frontiers in Plant Science* 2013, **4**.
7. Zhang S, Liu X, Jiang Q, Shen G, Ding W: **Legacy effects of continuous chloropicrin-fumigation for 3-years on soil microbial community composition and metabolic activity.** *AMB Express* 2017, **7:**178.
8. Wei Z, Yang X, Yin S, Shen Q, Ran W, Xu Y: **Efficacy of *Bacillus*-fortified organic fertiliser in controlling bacterial wilt of tomato in the field.** *Applied Soil Ecology* 2011, **48:**152-159.
9. Meena RS, Kumar S, Datta R, Lal R, Vijayakumar V, Brtnicky M, Sharma MP, Yadav GS, Jhariya MK, Jangir CK: **Impact of agrochemicals on soil microbiota and management: A review.** *Land* 2020, **9:**34.
10. Kostov O, Van Cleemput O: **Microbial activity of Cu contaminated soils and effect of lime and compost on soil resiliency.** *Compost science & utilization* 2001, **9:**336-351.
11. Wang Y, Li Q, Hui W, Shi J, Lin Q, Chen X, Chen Y: **Effect of sulphur on soil Cu/Zn availability and microbial community composition.** *J Hazard Mater* 2008, **159:**385-389.
12. Wang F, Zhou T, Zhu L, Wang X, Wang J, Wang J, Du Z, Li B: **Effects of successive metalaxyl application on soil microorganisms and the residue dynamics.** *Ecological Indicators* 2019, **103:**194-201.
13. Sederholm MR, Schmitz BW, Barberán A, Pepper IL: **Effects of metam sodium fumigation on the abundance, activity, and diversity of soil bacterial communities.** *Applied Soil Ecology* 2018, **124:**27-33.

14. Han L, Liu Y, Fang K, Zhang X, Liu T, Wang F, Wang X: **Azoxystrobin dissipation and its effect on soil microbial community structure and function in the presence of chlorothalonil, chlortetracycline and ciprofloxacin.** *Environmental Pollution* 2020, **257:**113578.
15. Liu K, Cai M, Hu C, Sun X, Cheng Q, Jia W, Yang T, Nie M, Zhao X: **Selenium (Se) reduces Sclerotinia stem rot disease incidence of oilseed rape by increasing plant Se concentration and shifting soil microbial community and functional profiles.** *Environmental Pollution* 2019, **254:**113051.
16. de Lima Procópio RE, da Silva IR, Martins MK, de Azevedo JL, de Araújo JM: **Antibiotics produced by *Streptomyces*.** *The Brazilian Journal of infectious diseases* 2012, **16:**466-471.
17. Yuan WM, Crawford DL: **Characterization of *streptomyces lydicus* WYEC108 as a potential biocontrol agent against fungal root and seed rots.** *Applied & Environmental Microbiology* 1995, **61:**3119-3128.
18. Mihaela U, Oana Alina B-S, Cătălina V, Vasilica S, Corina B, Călina Petruţa C: **The Potential of New *Streptomyces* Isolates as Biocontrol Agents Against Fusarium Spp.** *"Agriculture for Life, Life for Agriculture" Conference Proceedings* 2018, **1:**594-600.
19. Chen MC, Wang JP, Zhu YJ, Liu B, Yang WJ, Ruan CQ: **Antibacterial activity against *Ralstonia solanacearum* of the lipopeptides secreted from the *Bacillus amyloliquefaciens* strain FJAT-2349.** *Journal of Applied Microbiology* 2019, **126:**1519-1529.
20. Khan N, Maymon M, Hirsch A: **Combating *Fusarium* infection using *Bacillus*-based antimicrobials.** *Microorganisms* 2017, **5:**75.
21. Soledad ON, Florencia MM, Laura FM, Raúl DG, Balbina AA, Pía OF: **Potassium phosphite increases tolerance to UV-B in potato.** *Plant Physiol Biochem* 2015, **88:**1-8.
22. Norman DJ, Chen J, Yuen JMF, Mangravita-Novo A, Byrne D, Walsh L: **Control of Bacterial Wilt of Geranium with Phosphorous Acid.** *Plant Disease* 2006, **90:**798-802.
23. Cerqueira A, Alves A, Berenguer H, Correia B, Gómez-Cadenas A, Diez JJ, Monteiro P, Pinto G: **Phosphite shifts physiological and hormonal profile of Monterey pine and delays *Fusarium circinatum* progression.** *Plant Physiology and Biochemistry* 2017, **114:**88-99.
24. Costa BHG, de Resende MLV, Monteiro ACA, Ribeiro Júnior PM, Botelho DMdS, Silva BMd: **Potassium phosphites in the protection of common bean plants against anthracnose and biochemical defence responses.** *Journal of Phytopathology* 2018, **166:**95-102.
25. Felipini RB, Boneti JI, Katsurayama Y, Neto ACR, Veleirinho B, Maraschin M, Di Piero RM: **Apple scab control and activation of plant defence responses using potassium phosphite and chitosan.** *European Journal of Plant Pathology* 2016, **145:**929-939.
26. Niere JO, Deangelis G, Grant BR: **The effect of phosphonate on the acid-soluble phosphorus components in the genus *Phytophthora*.** *Microbiology* 1994, **140:**1661-1670.
27. Dempsey JJ, Wilson I, Spencer-Phillips PTN, Arnold D: **Suppression of the in vitro growth and development of Microdochium nivale by phosphite.** *Plant Pathology* 2018.
28. Albrigo L: **Effects of foliar applications of urea or nutriphite on flowering and yields of Valencia orange trees.** In *Proc Fla State Hort, Soc*. 1999: 1-4.

29. Mofidnakhaei M, Abdossi V, Dehestani A, Pirdashti H, Babaeizad V: **Potassium phosphite affects growth, antioxidant enzymes activity and alleviates disease damage in cucumber plants inoculated with *Pythium ultimum*.** *Archives of Phytopathology and Plant Protection* 2016, **49:**207-221.
30. Gómez-Merino FC, Trejo-Téllez LI: **Biostimulant activity of phosphite in horticulture.** *Scientia Horticulturae* 2015, **196:**82-90.
31. Metcalf WW, Wolfe RS: **Molecular Genetic Analysis of Phosphite and Hypophosphite Oxidation by *Pseudomonas stutzeri* WM88.** *Journal of Bacteriology* 1998, **180:**5547-5558.
32. Kehe J, Ortiz A, Kulesa A, Gore J, Blainey PC, Friedman J: **Positive interactions are common among culturable bacteria.** *bioRxiv* 2020**:**2020.2006.2024.169474.
33. Dundore-Arias JP, Felice LJ, Dill-Macky R, Kinkel LL: **Carbon amendments alter nutrient use and pathogen-suppressive potential of soil *Streptomyces*.** In *International Congress of Plant Pathology (ICPP) 2018: Plant Health in A Global Economy*. APSNET; 2018
34. Lu T, Zhang Q, Lavoie M, Zhu Y, Ye Y, Yang J, Paerl HW, Qian H, Zhu Y-G: **The fungicide azoxystrobin promotes freshwater *cyanobacterial* dominance through altering competition.** *Microbiome* 2019, **7:**128.
35. Hassan R, Shaaban MI, Abdel Bar FM, El-Mahdy AM, Shokralla S: **Quorum Sensing Inhibiting Activity of *Streptomyces coelicoflavus* Isolated from Soil.** *Frontiers in microbiology* 2016, **7:**659-659.
36. Sato I, Yoshida S, Iwamoto Y, Aino M, Hyakumachi M, Shimizu M, Takahashi H, Ando S, Tsushima S: **Suppressive potential of *Paenibacillus* strains isolated from the tomato phyllosphere against *fusarium* crown and root rot of tomato.** *Microbes and environments* 2014, **29:**168-177.
37. Yuliar, Nion YA, Toyota K: **Recent Trends in Control Methods for Bacterial Wilt Diseases Caused by *Ralstonia solanacearum*.** *Microbes & Environments* 2015, **30:**1-11.
38. Cao Y, Pi H, Chandrangsu P, Li Y, Wang Y, Zhou H, Xiong H, Helmann JD, Cai Y: **Antagonism of two plant-growth promoting *Bacillus velezensis* isolates against *Ralstonia solanacearum* and *Fusarium oxysporum*.** *Scientific reports* 2018, **8:**4360.
39. Kim J-h, Hancock IC: **Pellet forming and fragmentation in liquid culture of *Streptomyces griseus*.** *Biotechnology Letters* 2000, **22:**189-192.
40. Singh PP, Shin YC, Park CS, Chung YR: **Biological Control of *Fusarium* Wilt of Cucumber by Chitinolytic Bacteria.** *Phytopathology™* 1999, **89:**92-99.
41. Gao C-H, Cao H, Cai P, Sørensen SJ: **The initial inoculation ratio regulates bacterial coculture interactions and metabolic capacity.** *The ISME Journal* 2020.
42. Lewis JA: **Effect of Plant Residues on Chlamydospore Germination of *Fusarium solani* f. sp. phaseoli and on *Fusarium* Root Rot of Beans.** *Phytopathology* 1977, **77**.
43. Edgar RC: **UPARSE: highly accurate OTU sequences from microbial amplicon reads.** *Nature Methods* 2013, **10:**996.
44. Langille MGI, Zaneveld J, Caporaso JG, Mcdonald D, Dan K, Reyes JA, Clemente JC, Burkepile DE, Thurber RLV, Knight R: **Predictive functional profiling of microbial communities using 16S rRNA**

marker gene sequences. *Nature Biotechnology* 2013, **31:**814.

45. Caporaso JG, Kuczynski J, Stombaugh J, Bittinger K, Bushman FD, Costello EK, Fierer N, Pena AG, Goodrich JK, Gordon JI: **QIIME allows analysis of high-throughput community sequencing data.** *Nature Methods* 2010, **7:**335-336.
46. Desta M, Wang W, Zhang L, Xu P, Tang H: **Isolation, Characterization, and Genomic Analysis of *Pseudomonas* sp. Strain SMT-1, an Efficient Fluorene-Degrading Bacterium.** *Evolutionary Bioinformatics* 2019, **15:**1176934319843518.
47. Li X, Jousset A, de Boer W, Carrión VJ, Zhang T, Wang X, Kuramae EE: **Legacy of land use history determines reprogramming of plant physiology by soil microbiome.** *The ISME Journal* 2019, **13:**738-751.
48. Howard MM, Bell TH, Kao-Kniffin J: **Soil microbiome transfer method affects microbiome composition, including dominant microorganisms, in a novel environment.** *FEMS microbiology letters* 2017, **364:**fnx092.
49. Schloss PD, Westcott SL, Ryabin T, Hall JR, Hartmann M, Hollister EB, Lesniewski RA, Oakley BB, Parks DH, Robinson CJ: **Introducing mothur: Open-Source, Platform-Independent, Community-Supported Software for Describing and Comparing Microbial Communities.** *Applied & Environmental Microbiology* 2009, **75:**7537.
50. Bastian M, Heymann S, Jacomy M: **Gephi: an open source software for exploring and manipulating networks.** In *Third international AAAI conference on weblogs and social media*. 2009
51. Machado D, Andrejev S, Tramontano M, Patil KR: **Fast automated reconstruction of genome-scale metabolic models for microbial species and communities.** *Nucleic Acids Res* 2018, **46:**7542-7553.
52. Shannon P, Markiel A, Ozier O, Baliga NS, Wang JT, Ramage D, Amin N, Schwikowski B, Ideker T: **Cytoscape: A Software Environment for Integrated Models of Biomolecular Interaction Networks.** *Genome Research* 2003, **13:**2498-2504.

Figures

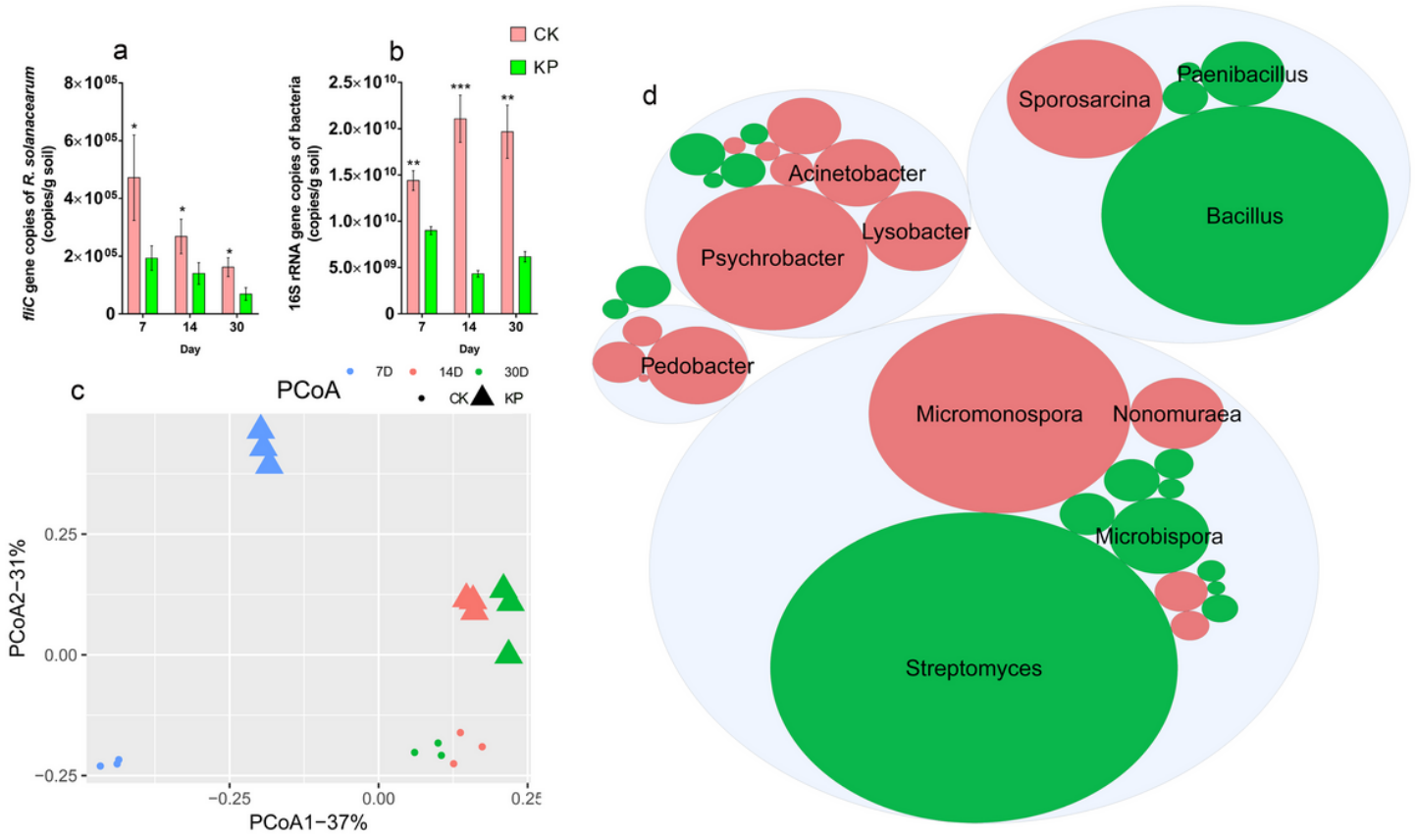

Figure 1

Effects of KP on the soil bacterial communities Copy numbers of fliC (a) and the 16S rRNA (b) between the KP treatment and the control. Statistical significance was determined based on Student's t test. * P < 0.05, ** P < 0.01, *** P < 0.001. Unless otherwise noted, "CK" and "KP" refer hereafter to control and KP treatment, respectively. (c) Principal coordinate analysis of the bacterial communities in the KP-treated soil and the control soil at different time points. (d) Significant differences in the relative abundance levels of bacterial genera between the KP treatment and the control at 7 days. The largest circles represent the phylum level. The inner circles represent the genus level. The colours of the circles indicate genera enriched in the KP treatment (green) or the control (red). The size of the circle represents the relative abundance of that genus.

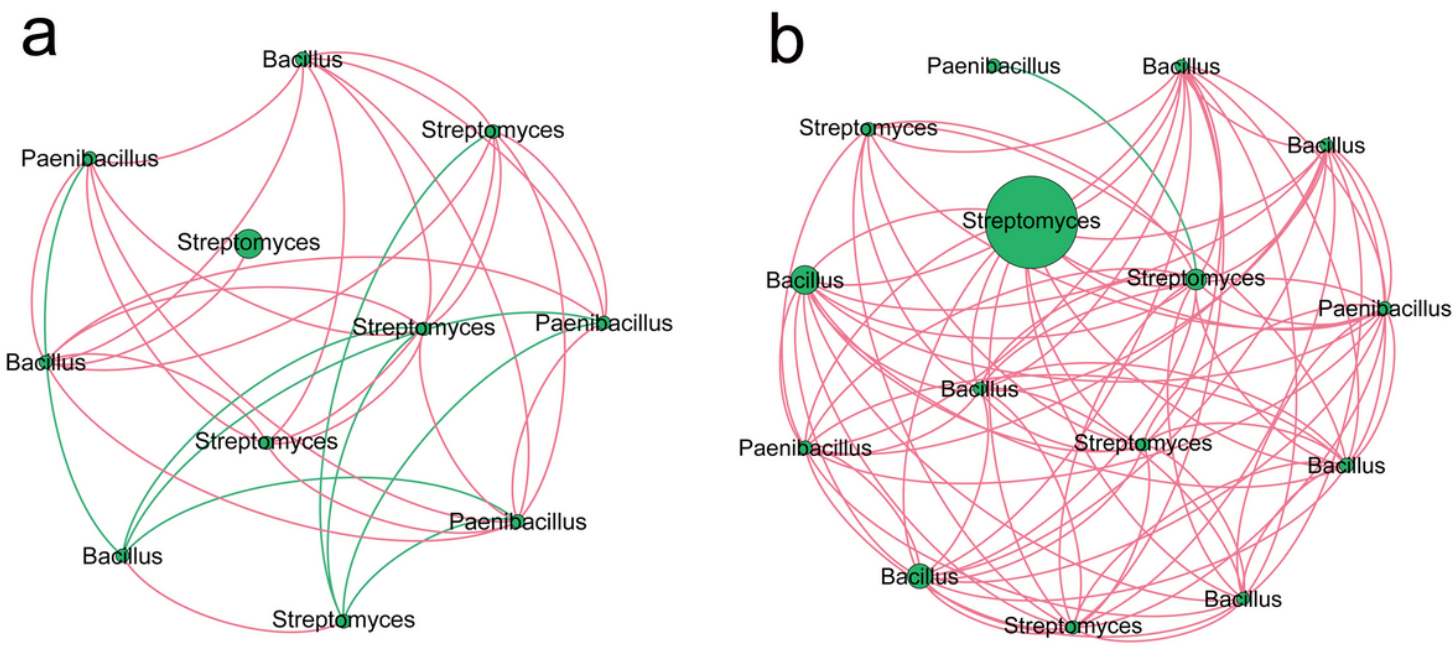

Figure 2

The associations among the hubs belonging to the potential antagonistic bacteria (Streptomyces, Paenibacillus and Bacillus) in the of control (a) and KP treatment networks (b). The green and red lines represent negative and positive links among bacteria, respectively. The node size represents the relative abundances of the node.

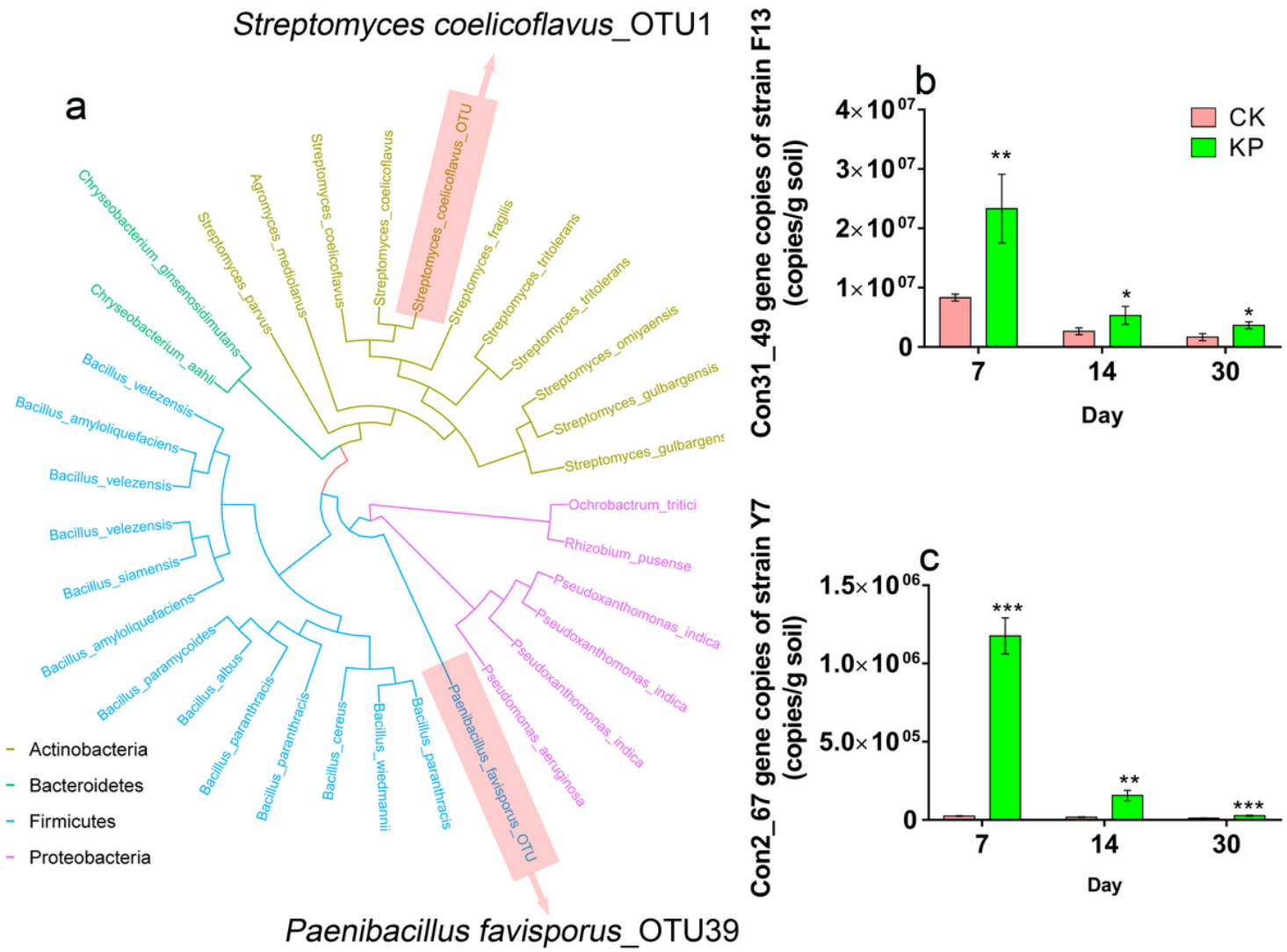

Figure 3

(a) The phylogenetic diversity of the isolates from the soil amended with KP at the species level. The isolates, for which the 16S rRNA sequences were clustered to sequences of target OTUs (Streptomyces and Paenibacillus) at 100% sequence similarity, are marked with a light red background. (b) Copy numbers of con31_49 of strain Streptomyces coelicoflavus F13 and (c) con2_67 of strain Paenibacillus favisporus Y7 in the soil amended with KP. Statistical significance was determined based on Student's t test. * $P < 0.05$, ** $P < 0.01$, *** $P < 0.001$. Statistical significance was determined by Student's t test. ** $P < 0.01$, *** $P < 0.001$.

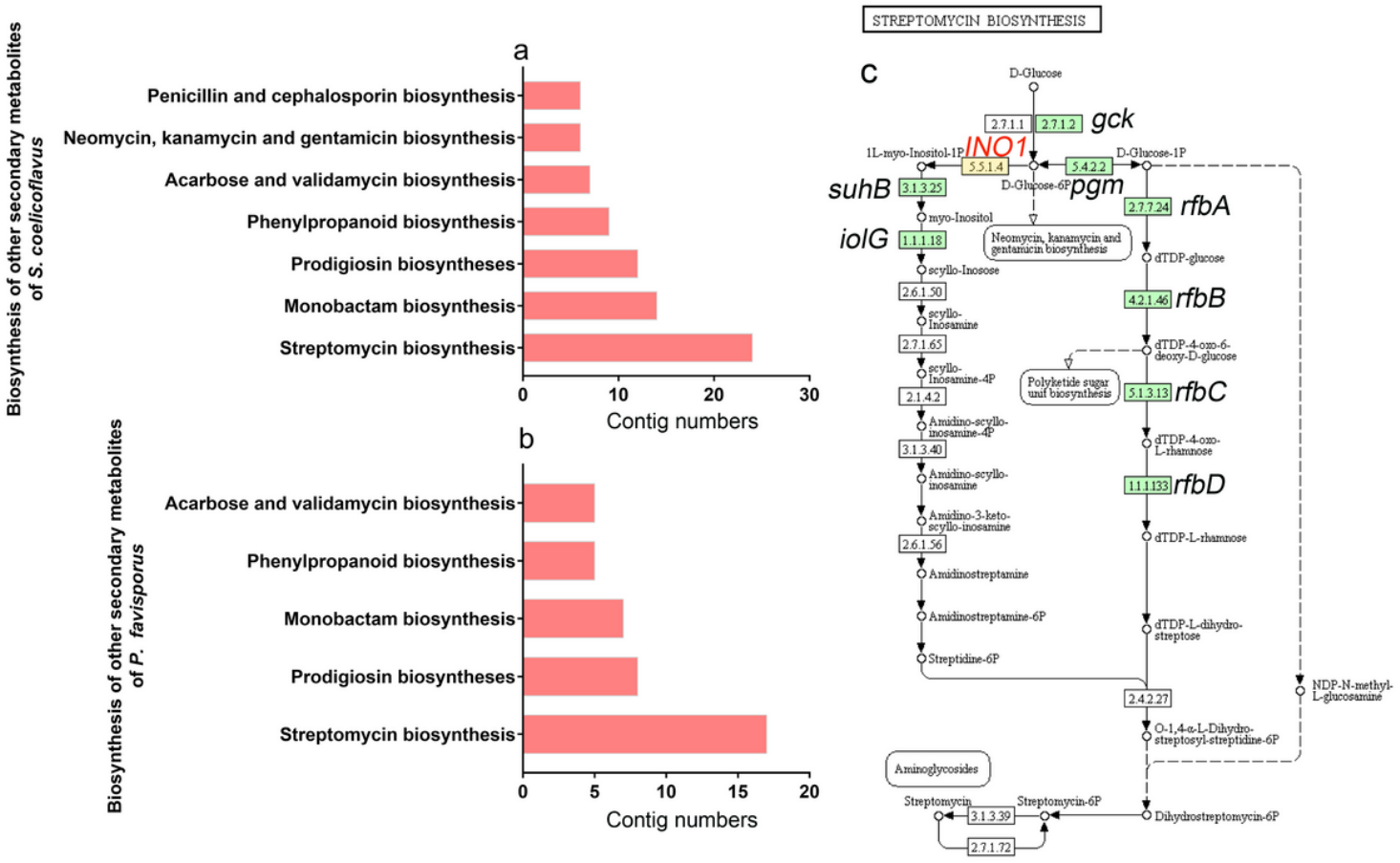

Figure 4

Functional analyses of the genomes of the isolates S. coelicoflavus F13 and P. favisporus Y7. The biosynthesis contig numbers of the other secondary metabolites in S. coelicoflavus F13 (a) and P. favisporus Y7 (b). The KEGG metabolic pathway of streptomycin biosynthesis in S. coelicoflavus F13 and P. favisporus Y7 (c). Gene labels marked with black or red font indicate that these genes were found in both isolates or only the isolate S. coelicoflavus F13, respectively.

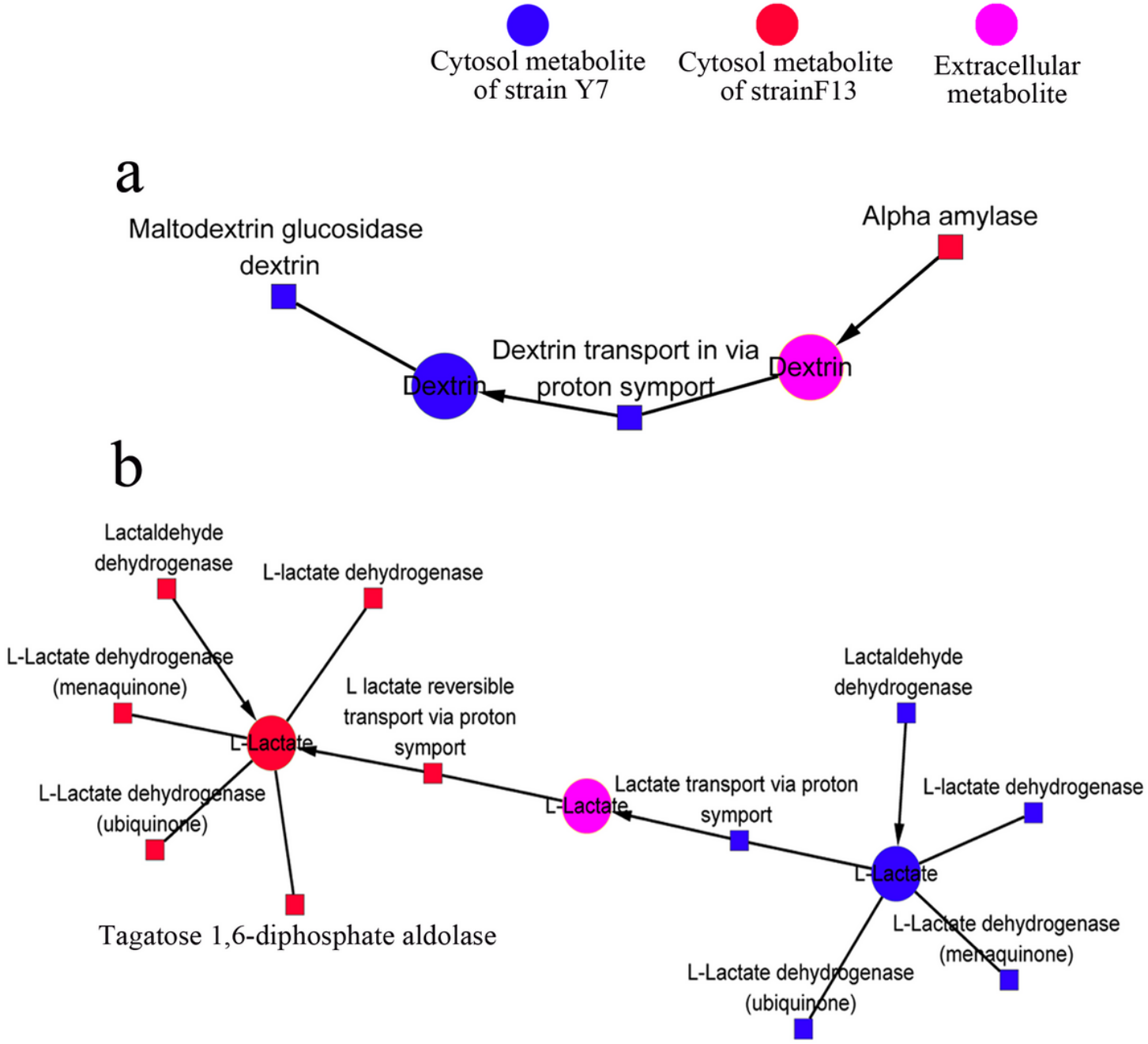

Figure 5

The potential cross-feeding metabolites dextrin (a) and L-lactate (b) in the genome-scale metabolic model between S. coelicoflavus F13 and P. favisporus Y7. Squares and circles represented reactions and metabolites, respectively. The green, red and pink circles represent the metabolites in the cytosol of strain Y7, cytosol of strain F13 and extracellular environments. The arrows and line segments represent the production and utilization of metabolites, respectively.

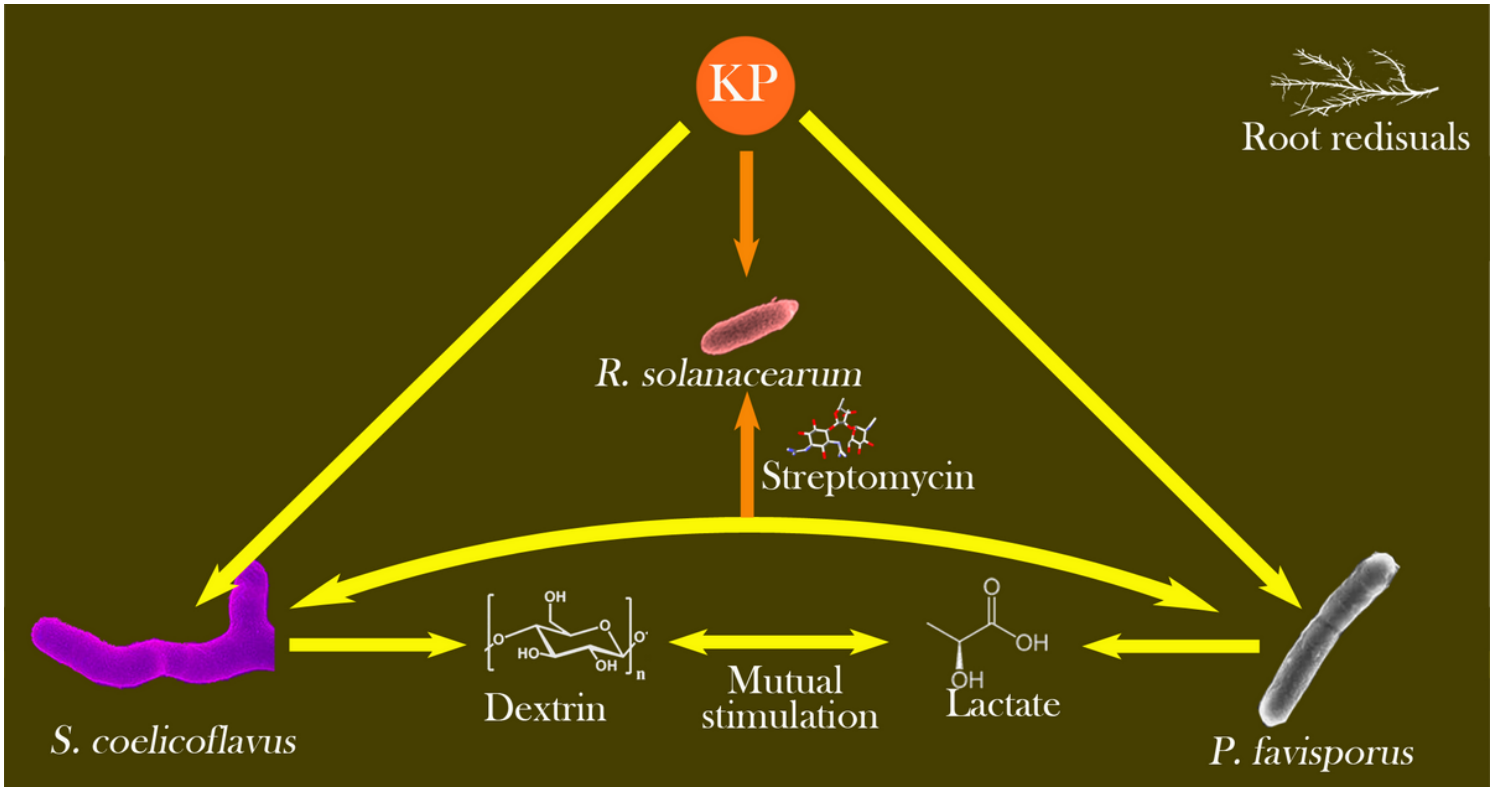

Figure 6

Proposed model for that the antagonistic bacteria Paenibacillus favisporus and Streptomyces coelicoflavus driven by KP, inhibiting the growth of R. solanacearum in soil under root residual conditions. The orange and yellow arrows represent R. solanacearum negatively affected by KP, P. favisporus and S. coelicoflavus, and P. favisporus and S. coelicoflavus positively affected by KP.

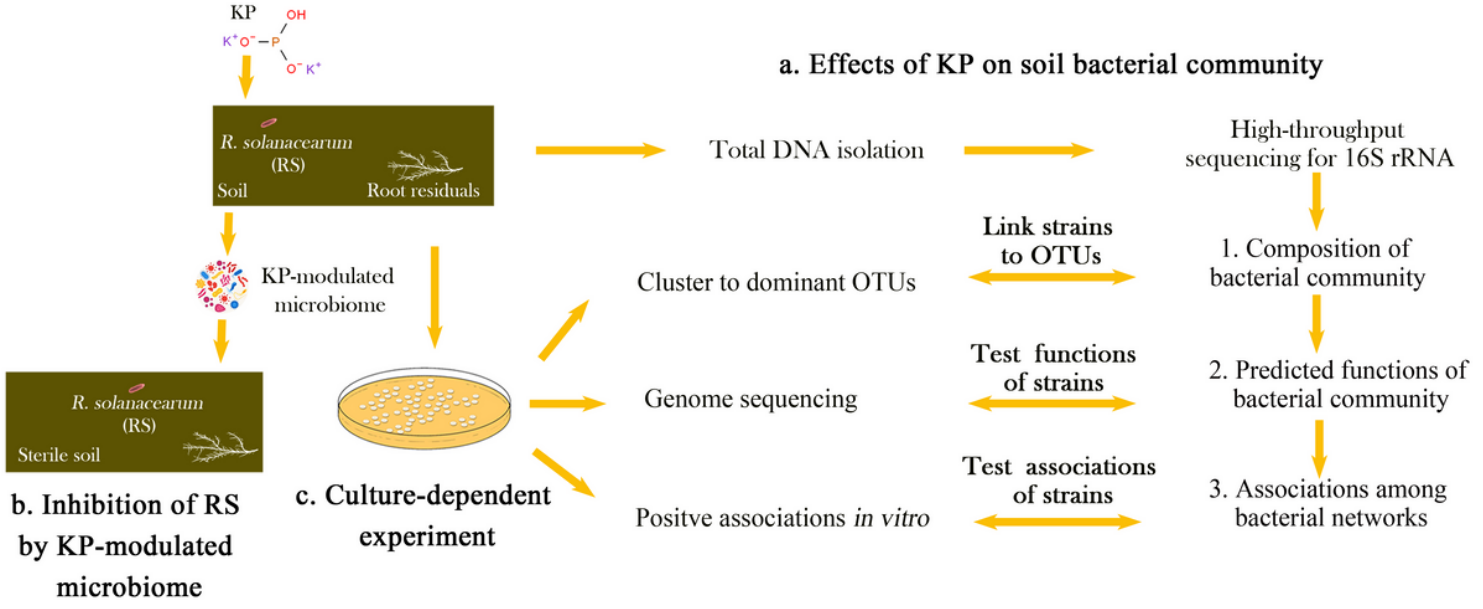

Figure 7

Flow diagram of the experimental design of this study

Supplementary Files

This is a list of supplementary files associated with this preprint. Click to download.

- manuscriptS17.docx